

Structural characterization and electronic structure of Li_3ClO glasses for solid-state Li-ion batteries

Young Won Choi^a, Moyses Araujo^b, Levente Vitos^{a,c,d} and Raquel Lizárraga^a

^aApplied Materials Physics, Department of Materials Science and Engineering, Royal Institute of Technology, Stockholm SE-100 44, Sweden

^bDepartment of Engineering and Physics, Karlstad University, Karlstad, Sweden

^cDepartment of Physics and Astronomy, Division of Materials Theory, Uppsala University, Box 516, SE-751 20 Uppsala, Sweden

^dResearch Institute for Solid State Physics and Optics, Wigner Research Center for Physics, Budapest H-1525, Hungary

ARTICLE INFO

Keywords:

Li-ion and Na-ion glasses
First principles characterization
Amorphous structure

ABSTRACT

Energy storage technologies that can meet the unprecedented demands of a sustainable energy system based on intermittent energy sources require new battery materials. We investigate high ionic conductors, Li_3ClO glasses. In the present work we use a first principles method to model the amorphous structure of the glass. We characterize the structure by means of radial distribution functions, radial distributions functions and coordination numbers. We compare to their crystalline counterparts. The electronic structure of the glass is compared to that of the crystalline material. The band gap of the glass appears to be slightly reduced compared to that of the crystal. We also investigate the chemical stability of the glass against Li metal electrode. The electrochemical stability of the glassy electrolyte is evaluated against Li metal.

1. Introduction

The lithium-ion battery (LIB) is the fastest growing and most promising battery for a broad range of applications, e.g. portable electronics, robotics and all-electric vehicles. Its most common design consists of a graphite anode, a Li metal oxide cathode and an electrolyte made of Li salt and an organic solvent. The electrolyte provides the conductive medium, in which the Li ions travel back and forth from one electrode to the other during discharge and charge. Presently, three types of LIBs are envisioned as the next generation Li-ion battery, namely, metal-air, multi-valent cation and all-solid state batteries [13]. The latter is a very promising battery that has many advantages [8, 6] and it is currently considered the next step on major OEM's roadmaps [11]. Firstly, the all-solid-state battery can be made thinner and safer than conventional LIBs, because it does not need a separator and it does not use flammable liquid materials for the electrolyte that are susceptible to dangerous leaks. Secondly, the solid-state electrolyte can withstand voltages up to 10 V which can enable high voltage cathodes, and consequently increase the energy density capacity of the battery by 20-50 %. Moreover, solid electrolytes usually show excellent storage stability and very long life [7].

The challenge of the all-solid-state battery is to increase ionic conductivity to be comparable or even better than that of conventional liquid electrolytes (typically around 10^{-3} S/cm at room temperature [8]). Solid electrolyte materials exhibit rather low ionic conductivity ranging from 10^{-8} to 10^{-5} S/cm (halides), 10^{-5} to 10^{-3} S/cm (oxides), 10^{-7} to 10^{-3} S/cm (sulfides) and 10^{-7} to 10^{-4} S/cm (hydrides) [6]. Currently, ceramics, sulfides, solid polymers, glasses and composites

of ceramics or glasses are materials proposed for solid-state electrolyte technology. Glasses have been known for a while to be fast ionic conducting materials, however research efforts have been concentrated mostly on synthesis and optimization of the thermal properties [4].

Recently, Braga et al. proposed and patented a new all-solid state battery architecture based on Li^+ or Na^+ glassy electrolytes [13, 1, 2, 3]. One of the major breakthroughs of this new battery is the fact that, it can be realized using Na which is abundant, inexpensive and capable of promoting sustainable use of raw materials. Furthermore, it may be made without cobalt in the cathode, which is an advantage because cobalt presents several unresolved issues regarding health [5, 19] and irresponsible mining practices [14]. This battery promises to provide 2-3 times the energy storage capacity of a comparable LIB and most importantly it appears not to form dendrites, which are associated to short circuits in LIBs.

In the present study we investigate the amorphous structure of Li_3ClO glass and its electronic structure and we compare with its crystalline counterpart. The paper is organized as following. In section 2 we discuss the methodology and computational methods used in this investigation. Section 3 presents the results and discussions. Finally in section 4 we present the conclusions of our study.

2. Methodology

Models of the amorphous structure have been generated by means of the stochastic quenching method (SQ) [17, 16]. The method is based on Density Functional Theory [15, 23] and it has been used extensively in the past to study amorphous systems e.g. amorphous alumina [21], amorphous graphite [18], amorphous YCrO_3 [9, 22], amorphous GdRE_2 [20], etc. The size of the cell was carefully tested and models with 100, 250 and 500 atoms were generated. We did not

*Corresponding author

✉ ywchoi@kth.se (Y.W. Choi); Moyses.Araujo@kau.se (M. Araujo);

levente@kth.se (L. Vitos); raqli@kth.se (R. Lizárraga)

ORCID(s): 0000-0002-6794-6744 (R. Lizárraga)

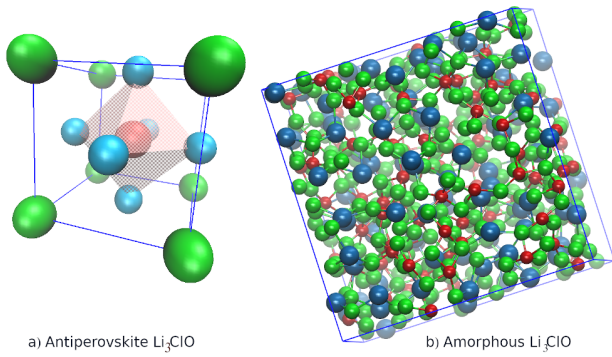


Figure 1: Antiperovskite Li_3ClO and Li_3ClO amorphous structures. The model of the amorphous structure of Li_3ClO was obtained using SQ method and cell of 500 atoms. Red, blue and green balls represent Cl, O and Li atoms respectively.

observed significant differences between the 250-atoms and 500-atoms cell. The equilibrium density of the glass was determined to be 1.63 g/cm^3 which is approximately 18% lower than the crystalline counterpart.

2.1. Computational details

The Vienna ab initio Simulation Package [26] (VASP) was used during the quenching. The Perdew-Burke-Ernzerhof (PBE) implementation of the exchange-correlation functional was used to generate the models of amorphous structures [25] Due to the GGA's well known failure to describe the band gap correctly, we also performed GW0 and HSE calculations. The eigenstates of the electron wave functions were expanded on a plane-waves basis set using pseudopotentials to describe the electron-ion interactions within the projector augmented waves approach (PAW)[12].

The convergence criterion for the electronic self-consistent cycle was fixed at 10^{-7} eV per cell and for the relaxation of the forces on all ions, it was 10^{-5} eV/Å. Calculations were performed at the Γ k-point with a cutoff energy of 350 eV. Calculations of antiperovskite structure were performed utilizing a k-point mesh of $12 \times 12 \times 12$, except when density of states (DOS) was calculated, in which case a $22 \times 22 \times 22$ was used. Structural optimizations were performed by using a standard conjugate gradient method during the stochastic quenching procedure.

3. Results and Discussion

3.1. Amorphous structure

Fig. 2 shows selected radial distribution functions (RDFs) for crystalline and amorphous Li_3ClO . In all cases, the first peak of the RDFs of the amorphous structure are shifted towards lower values than those of the crystalline structure. These is clearly reflected in the bond distances. Table 2 lists the bond distances for both crystalline and amorphous structures. In all cases this distance is shorter in the glass. In particular, the main peak of $g_{\text{O-O}}$ moves from 3.9 Å in the crystalline structure to 3.1 Å in the glass and a small peak develops at 1.5 Å. This small peak has been associated to oxy-

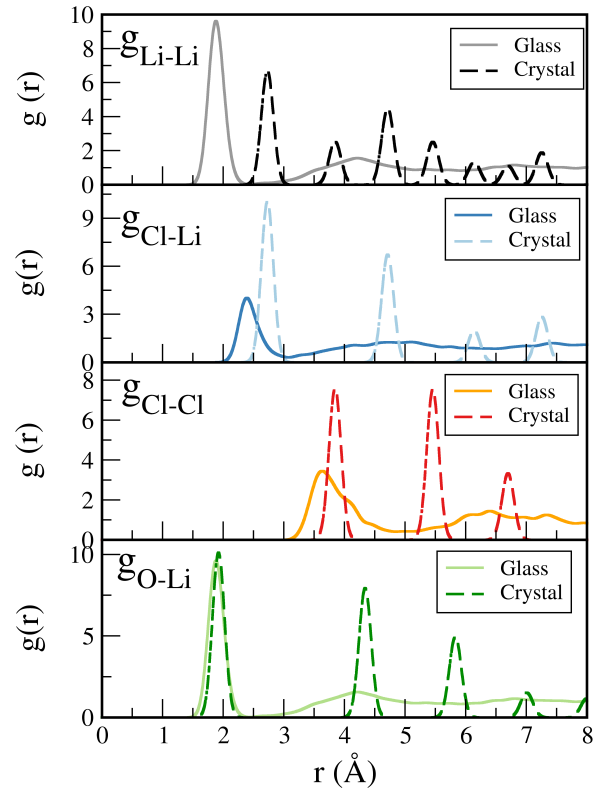


Figure 2: Radial distribution function of crystal and amorphous structure of Li_3ClO . (a) denote Li-Li, Cl-Li, Cl-Cl, and Cl-O pairs and (b) O-O and Cl-O pairs.

gen molecules impurities and have been observed before in other amorphous materials such as amorphous alumina [10].

Table 1

Bond distance in crystalline and amorphous Li_3ClO .

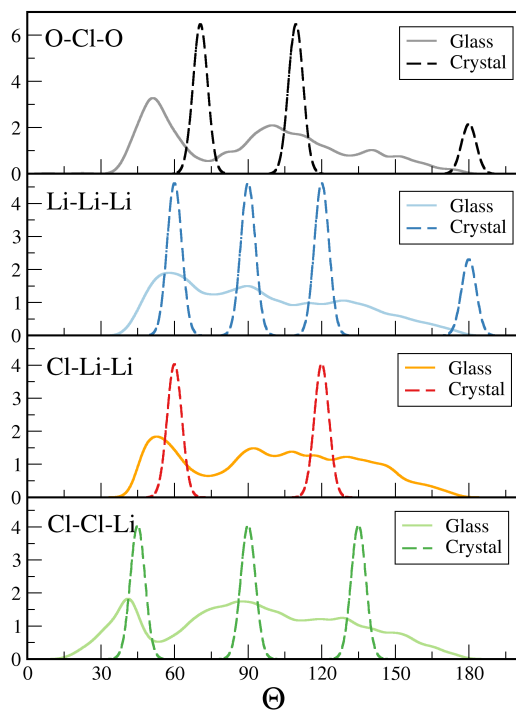
Bond	Shortest Distance (Å)	
	Crystalline	Amorphous
O-O	3.91	1.54
O-Li	1.96	1.79
O-Cl	3.39	3.25
Li-Li	2.76	2.18
Li-Cl	2.76	2.31
Cl-Cl	3.91	3.41

Coordination numbers are listed in Table 1. It is shown that most of pairs have smaller coordination number in amorphous state compared to crystalline one. For example, the coordination number of O-O pair is reduced from 6 into 4.4 by amorphization. However, O-Li coordination number increases from 6 to 10.25, which means O atom went to Li atom from O atom.

Fig.3 displays the angular distribution function (ADFs) of crystal and amorphous state of Li_3ClO . It is shown that the O-O-Li angle which is originally located at 0° in the crystalline structure changes into 32° and the O-Li-Li angle

Table 2Coordination numbers of crystalline and glassy Li₃ClO.

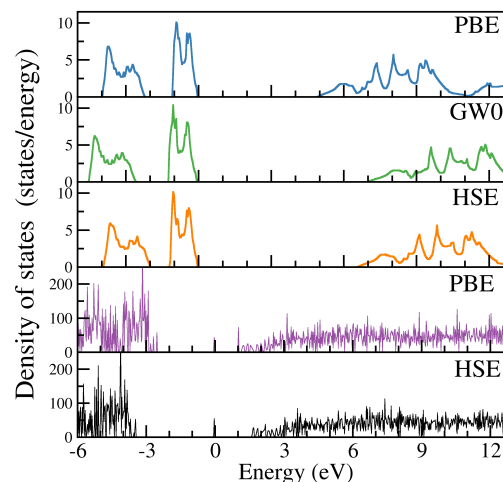
Bond	Crystalline	Amorphous
O-O	6	4.4
O-Li	6	10.25
O-Cl	8	4.6
Li-Li	14	10.57
Li-Cl	4	2.95
Cl-Cl	6	3.4

**Figure 3:** Selected angular distribution function of crystal and amorphous structure of Li₃ClO. Full- and dashed-lines represent amorphous and crystalline structure, respectively.

which is positioned at 0°, 45°, and 90° changes into 32° and 42°. Therefore, their angle becomes smaller into an acute angle. On the other hand, the O-Cl-Li angle which is located at 36° in crystalline state becomes 31°, and thus its change is small compared to other angles presented in the figure.

3.2. Electronic structure

Fig. 4 shows the density of states (DOS) of crystalline and glassy Li₃ClO. From top to bottom the figure displays DOS for: anti-perovskite Li₃ClO as calculated by PBE, GW0 and HSE and glassy Li₃ClO PBE and HSE. The calculated band gap of crystalline Li₃ClO as obtained by PBE, GW0 and HSE is 4.84 eV, 6.9 eV and 6.48 eV, respectively. These results are in good agreement with other values found in the literature; 6.44 [13] and 5 eV [24]. The band gap of the amorphous system is in comparison relatively smaller, 3.55 eV for PBE and 5.03 for HSE. However we observe that the

**Figure 4:** Density of states of crystalline and amorphous Li₃ClO for several exchange and correlation functionals. From top to bottom: crystalline (PBE), crystalline (GW0), crystalline (HSE), glass (PBE), glass (HSE).

valence band shifts to higher energy levels.

4. Conclusions

We have investigated Li₃ClO in the amorphous and crystalline state by means of ab initio calculations. Models of the amorphous structure of Li₃ClO glass were generated by the stochastic quenching method. The amorphous structures were characterized by means of radial distributions functions and angle distribution functions. Coordination numbers and bond lengths were also obtained from the simulations. These materials are insulators in both the crystalline state and as a glass. The density of states was investigated using PBE, GW0 and the hybrid HSE functionals. As expected the band gap obtained by PBE is smaller than both GW0 and HSE results.

References

- [1] et al., B., 2016. Glass-amorphous alkali-ion solid electrolytes and their performance in symmetrical cells. *Energy Environ. Sci.* 9, 948.
- [2] et al., B., 2017a. *Energy Environ. Sci.* 10, 331.
- [3] et al., B., 2018. *J. Am. Chem. Soc.* 140, 6343–6352.
- [4] et al., K., 1992. *Sol. States Ionics* 53, 1183.
- [5] et al., L., 2004. *Occup. Environ. Med.* 61, 877–885.
- [6] et al., M., 2017b. *Nature Reviews Materials* 2, 16103.
- [7] et al., T., 2013. *Acta Mater.* 61, 759–770.
- [8] et al., W., 2015. *Nature Mater.* 14, 1026.
- [9] Araujo, M., Nagar, S., Ramzan, M., Shukla, R., Jayakumar, O.D., Tyagi, A.K., Liu, Y., Chen, J., Glans, P.A., Chang, C., Blomqvist, A., Lizárraga, R., Holmström, E., Belova, L., Guo, J., Ahuja, R., Rao, K.V., 2014. *Sci. Rep.* 4, 4686.
- [10] Århammar, C., Pietzsch, A., Bock, N., Holmström, E., Araujo, C.M., Gräsjö, J., Zhao, S., Green, S., Peery, T., Hennies, F., Amerioun, S., Föhlisch, A., Schlappa, J., Schmitt, T., Strocov, V.N., Niklasson, G.A., Wallace, D.C., Rubensson, J.E., Johansson, B., Ahuja, R., 2011. *Proc. Nat. Aca. Sci. Amer* 108, 6355.

- [11] author, . European Battery Cell R& I Workshop. European Commission (2018) Brussels. Final Report. European Battery Alliance.
- [12] Blöchl, P.E., 1994. Phys. Rev. B 50, 17953.
- [13] Braga, M.H., Ferreira, J.A., Stockhausen, V., Oliveira, J.E., El-Azab, A., 2014. Novel Li_3ClO based glasses with superionic properties for lithium batteries. J. Mater. Chem. A 2, 5470–5480.
- [14] guardian, T., . <https://www.theguardian.com/global-development/2019/dec/16/apple-and-google-named-in-us-lawsuit-over-congolese-child-cobalt-mining-deaths>.
- [15] Hohenberg, P., Kohn, W., 1964. Phys. Rev. B 136, 864.
- [16] Holmström, E., Bock, N., Perry, T., Chilsom, E., Lizárraga, R., De Lorenzi, G., Wallace, D., 2010. Phys. Rev. B 82, 024203.
- [17] Holmström, E., Bock, N., Perry, T., Lizárraga, R., De Lorenzi, G., Chisolm, E., Wallace, D., 2009. Phys. Rev. E 80, 51111.
- [18] Holmström, E., Fransson, J., Eriksson, O., Lizárraga, R., Sanyal, B., Bhandary, S., G, Katsnelson, M., 2011. Phys. Rev. B 84, 245414.
- [19] Holmström, E., Lizárraga, R., Linder, D., Salmasi, A., Wang, W., Kaplan, B., Mao, H., Larsson, H., Vitos, L., 2018. Appl. Mater. Today 12, 322–329.
- [20] Lizárraga, R., 2016. Phys. Rev. B 94, 174201.
- [21] Lizárraga, R., Holmström, E., Parker, C., Arrouvel, C., 2011. Phys. Rev. B 83, 094201.
- [22] Lizárraga, R., Ramzan, M., Araujo, M., Blomqvist, A., Ahuja, R., Holmström, E., 2012. Europhys. Lett. 99, 57010.
- [23] Martin, R.M., 2004. Electronic Structure: Basic Theory and Practical Methods. Cambridge University Press.
- [24] Mo, Y., Ong, P., Ceder, G., 2012. First principles study of the $\text{Li}_1\text{Ogep}_2\text{S}_12$ lithium super ionic conductor material. Chem. Mater. 24, 15–17.
- [25] Perdew, J.P., Burke, K., Ernzerhof, M., 1996. Generalized gradient approximation made simple. Phys. Rev. Lett. 77, 3865–3868.
- [26] Vasp, . <http://cms.mpi.univie.ac.at/vasp/>.